Desorption of n-alkanes from graphene: a van der Waals density functional study

Desorption of n-alkanes from graphene: a van der Waals density functional study

Elisa Londero, Emma K. Karlson, Marcus Landahl, Dimitri Ostrovskii, Jonatan D. Rydberg, and Elsebeth Schröder*
Microtechnology and Nanoscience, MC2, Chalmers University of Technology, SE-412 96 Göteborg, Sweden
(Dated: July 7, 2012, Submitted to Journal of Physics: Condensed Matter)

A recent study of temperature programmed desorption (TPD) measurements of small linear alkane molecules (n-alkanes, with formula C_NH_{2N+2}) from C(0001) deposited on Pt(111) shows a linear relationship of the desorption energy with increasing n-alkane chain length N. We here present a van der Waals density functional study of the desorption barrier energy of the ten smallest n-alkanes (of carbon chain length $N = 1$ to 10) from graphene. We find linear scaling with N, including a nonzero intercept with the energy axis, i.e., an offset at the extrapolation to $N = 0$. This calculated offset is quantitatively similar to the results of the TPD measurements. From further calculations of the polyethylene polymer we offer a suggestion for the origin of the offset.

PACS numbers: 31.15.E-,71.15.Mb,71.15.Nc

I. INTRODUCTION

The increasing use of molecules on graphene and graphite surfaces for industrial applications calls for an improved atomic-scale understanding of the adsorption/desorption structure and process. The n-alkanes[1] are linear chains of hydrocarbons, short versions of the polyethylene (PE) polymer. Using temperature-programmed desorption (TPD) Tait et al. (Ref. 1) measured the desorption energy and desorption rate pre-exponential factor of n-alkanes on graphene deposited on a Pt(111) substrate. The n-alkanes measured were short, with the number of C atoms $N \leq 10$. The desorption of n-alkanes from graphite surfaces was also measured by Paserba and Gellman [2–4], and from various other surfaces by a number of other groups [5], the surface materials including metals (Ag, Au, Cu, Pt, Ru), oxides (Al_2O_3, MgO), and semiconductors (Si).

In most of the alkane desorption measurements the desorption energy was found to scale linearly with N for the short n-alkanes, but with a non-zero intercept with the axis of the desorption energy. The value found for this offset at $N = 0$ was sometimes found to be unphysically large, several times larger than the scaling coefficient. In another study Tait et al. [6, 7] analyzed their own data for n-alkane on MgO(100) desorption. They allowed the desorption prefactor to vary with chain length and found the desorption energy offset to be non-vanishing but small, of the size of or smaller than the scaling coefficient. When the same group of authors analyzed their data of n-alkanes on Pt(111) and on graphene (and also re-analyzed data from a number of studies by other groups for some of the above-mentioned surfaces) they found similar non-vanishing but small offsets for those desorption systems.

In this paper we use the first-principles van der Waals (vdW) density-functional method [8, 9], vdW-DF, to determine the n-alkane adsorption energy on graphene at low coverages for short alkane chains ($N \leq 10$). This adsorption energy can be compared with the experimentally determined desorption barrier energy values. As in the experimental studies in Refs. 1, 6, and 7 we find a close-to-linear growth in adsorption energy E_a with chain length N, with a non-vanishing but small offset when extrapolated to $N = 0$

$$E_a = 7.23N + 6.44 \text{ [kJ/mol]}. \quad (1)$$

Here and below we use the term adsorption energy (E_a) for the energy found in our theory calculations. This corresponds to the desorption energy E_0 of isolated alkane molecules on graphene. By E_d we denote the experimental desorption energy, or desorption barrier, of an alkane molecule from partly covered graphene. In parts of the literature E_d is instead denoted $\Delta E^{\ddagger}_{\text{des}}$.

Contrary to analysis of the experiments, our calculations of the adsorption/desorption energy do not involve an assessment of the desorption prefactor. Our values of E_a are simply found from the differences in total energies of the system in the adsorbed and the desorbed states.

The outline of the paper is as follows. In Section II we describe the method of computation, including unit-cell choices and a discussion of both effective unit-cell coverages and our handling of direct vdW interactions between the repeated images of the adsorbates. Section III presents our results and discussions, including a discussion of the experimental analysis that permits our comparison. Section IV contains our summary.

II. METHOD OF COMPUTATION

Our interest in the alkane desorption was sparked by the TPD experiments of Tait et al. [1] and their analysis leading to the experimentally determined desorption energy.

The n-alkanes are linear, saturated hydrocarbon chains absent of branches, with the general formula C_NH_{2N+2},

*Corresponding author; Electronic address: schroder@chalmers.se

[1] Linear alkane isomers without branches are called "normal" alkanes, shortened n-alkanes.

$N > 0$. Very long such chains (in principle infinitely long) are known as the PE polymer. In this paper we analyze the adsorption on graphene of the ten smallest n-alkanes ($1 \leq N \leq 10$), of H_2, and of PE, all in the stretched form, which is the trans conformation.

A. Unit cell choices and code convergence

We determine the adsorption energy by use of first-principles density functional theory (DFT), employing the vdW-DF method [8, 9] as detailed in several other publications [10–12] but here with the vdW interaction treated fully selfconsistently. We calculate the total energies of the adsorption system using the DFT program GPAW [13, 14] with vdW-DF in a fast-Fourier-transform implementation [15].

We first use a set of vdW-DF calculations to determine the optimal lattice constants of isolated graphene, $a_g = \sqrt{3}\,a_0$, with $a_0 = 1.43$ Å. Then for each of the adsorbed alkane molecules we determine the optimal positions of the atoms by letting the molecules relax (using vdW-DF) to minimize the Hellmann-Feynman forces. These are derived from gradients in the self-consistently determined electron density. We relax the positions of the alkane atoms until the remaining force on each of the alkane atoms is less than 0.01 eV/Å. This optimization adjusts the intramolecular bond lengths to the most favorable value in the adsorption state. After this optimization we obtain the total energy of the adsorbate-graphene system, $E_{\rm near}^{\rm vdW\text{-}DF}$.

Figure 1 illustrates the adsorbed n-pentane molecule on graphene, and the unit cell used in our calculations for $N = 5$. We model the adsorption system by means of an orthorhombic unit cell, periodically repeated in all directions. Table I lists the lateral sizes, i.e., the extension in the plane of graphene, for all the unit cells used in the vdW-DF adsorption-energy studies.

The unit cells contain sufficient space in lateral directions to limit the mutual vdW coupling [21] between the repeated images of the n-alkane molecules. In addition, we use a simple procedure [12, 22, 23] to ensure that the direct vdW interactions between the adsorbate images are exactly compensated and potential grid and noise effects are minimized. This procedure involves calculating the vdW-DF energy $E_{\rm far,froz}^{\rm vdW\text{-}DF}$ of an intermediate state — with the adsorbate lifted far from the graphene while frozen in its adsorbate morphology — in the *same* unit cell as was used for $E_{\rm near}^{\rm vdW\text{-}DF}$. This calculation scheme is motivated below.

The introduction of ∼19 Å of vacuum above the adsorbed alkane ensures that interactions across unit cell boundaries in the direction perpendicular to graphene can be ignored in the evaluation of $E_{\rm near}^{\rm vdW\text{-}DF}$. With unit cell height 23 Å the maximum possible separation is ∼11 Å. This is almost but not quite sufficient for the alkane to count as fully desorbed on a meV scale and $E_{\rm far,froz}^{\rm vdW\text{-}DF}$ is thus affected. In the discussion section we argue that this leads to an underestimate of the adsorption energy, by about 4.5%; we judge that this is a fair compromise between computational cost and accuracy.

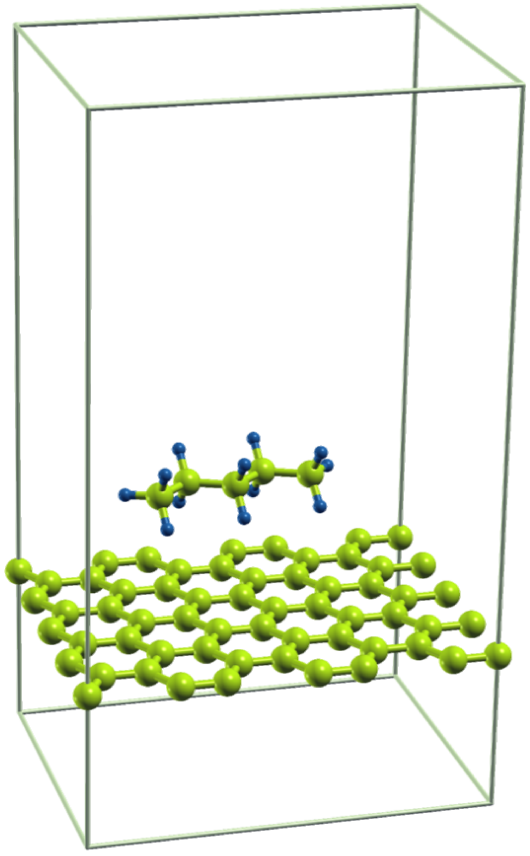

FIG. 1: Illustration of n-pentane ($N = 5$) adsorbed on graphene. One unit cell is shown including a repetition of the graphene C atoms that are positioned on the unit cell boundary. C (H) atoms are represented by large (small) spheres. Figure created using XCrySDen [16].

The GPAW code is an all-electron DFT code based on projector augmented waves [24] (PAW) and using finite differences. We choose the real-space grid for representing the wavefunctions in the PAW procedure to have a distance less than 0.11 Å between grid points. The pseudo electron density uses the same grid. Additional grid points are added by interpolation to obtain a finer grid with half the grid spacing [14]; in our calculations the grid spacing for the pseudo electron density is thus less than 0.055 Å. This is less than the GPAW default of about 0.2 Å for the wave function grid spacing, leading to about 0.1 Å grid spacing for the pseudo density. The use of a dense electron density grid is important for the quality of the evaluation of the nonlocal correlation contribution [25, 26].

The Brillouin zone of the unit cell is sampled according to the Monkhorst-Pack scheme by means of a 2×2×1 k-point sampling. Increasing the k-point sampling to 4×4×1 changes E_a by less than 0.7 meV per molecule

TABLE I: Adsorption (desorption) energies from theory (E_a) and experiment (E_d and E_0), center-of-mass distance from graphene d_{cm}, area A of one alkane molecule in a full monolayer (ML), unit cell used in calculations, and estimated unit-cell coverages $\theta_{\rm uc}$, for the small n-alkanes (C_NH_{2N+2}, $N = 1-10$). In our calculations we use orthogonal unit cells of height 23 Å (perpendicular to the plane of graphene) and a graphite lattice vector $a_g = \sqrt{3}\,a_0$ with $a_0 = 1.43$ Å. The experimental values of E_0 — corresponding to the limit of 0 ML coverage and no defect sites — is found from Eq. (9) with the use of parameters given in Table IV of Ref. 1. The unit-cell coverage for the polyethylene (PE) study is found from an estimate of the PE-PE bonding separation in the PE crystal, as described in the text.

		This work					Experiments		
	N	Unitcell	$\theta_{\rm uc}$ [ML]	d_{cm} [Å]	E_a [kJ/mol]	E_a [eV]	A [Å^2]	E_d(0.5 ML) [kJ/mol]	E_0 [kJ/mol]
H_2	0	$2\sqrt{3}\times 3$		3.39	6.8	0.070			
methane	1	$3\sqrt{3}\times 3$	0.16	3.64	14.6	0.152	15[a]	14.1	13.6
ethane	2	$3\sqrt{3}\times 3$	0.22	3.80	20.9	0.216	20.9[b]	24.6	23.8
propane	3	$3\sqrt{3}\times 3$	0.28	3.90	27.7	0.288	27[a]	32.1	30.6
$n-$butane	4	$3\sqrt{3}\times 4$	0.26	3.97	34.6	0.358	32.7[c]	40.8	38.9
$n-$pentane	5	$3\sqrt{3}\times 4$	0.31	3.86	42.8	0.443	39[a]		
$n-$hexane	6	$4\sqrt{3}\times 4$	0.26	3.96	49.6	0.514	45.6[d], 44.8[e]	63.0	60.3
$n-$heptane	7	$4\sqrt{3}\times 4$	0.30	3.90	57.7	0.598	51.6[f]		
$n-$octane	8	$5\sqrt{3}\times 4$	0.27	3.89	65.5	0.679	57.2[f], 57.7[d], 56.2[e]	72.6	71.0
$n-$nonane	9	$5\sqrt{3}\times 4$	0.30	3.87	73.0	0.757	63.5[f]		
$n-$decane	10	$5\sqrt{3}\times 4$	0.32	3.86	80.3	0.832	69.0[f], 69.7[d], 68.9[e]	91.4	84.5
polyethylene	(1)	$5\sqrt{3}\times 1$	0.21	3.83	7.2[g]	0.074[g]			

[a] Linear interpolation of the experimental data available for other values of N, $A(N) \approx 9 + 6N$ Å^2.

[b] Neutron diffraction data at submonolayer coverage, Ref. 17.

[c] Neutron diffraction data at 11 K, Ref. 18.

[d] X-ray diffraction data at submonolayer coverage, Ref. 19.

[e] Neutron diffraction data at submonolayer coverage, Ref. 19.

[f] X-ray diffraction data, Ref. 20.

[g] E_a per C atom in PE. Each unit cell has two units of CH_2.

(0.07 kJ/mol). We further make sure that the individual GPAW calculation is accurately converged with respect to the internal GPAW evaluation of the total energies. This step is to control the noise level in the electron density variation. We impose a convergence threshold such that the total energy changes less than 0.1 meV per unit cell, or less than approximately 10^{-6} eV per atom in the unit cell, in the last three iterations of the GPAW self-consistency scheme. This convergence threshold is several orders of magnitude smaller than the default settings of GPAW.

B. Unit-cell coverages

The coverage θ is an important parameter in the experimental characterization. One monolayer (ML) is a one-molecule thick coating of a surface, as found by experiments. The coverage of molecular adsorbates on the graphene substrate is specified as a fraction of a full ML. To assist comparisons between experiments and theory, we provide estimates of the effective unit-cell coverages, $\theta_{\rm uc}$, that characterize our above-described calculational choices. These $\theta_{\rm uc}$ estimates are listed in Table I.

Couto et al. [27] found by means of STM that for various n-alkanes adsorbed on graphite the coating layer is highly ordered. The ordering at such high coverage is affected both by the adsorbate-adsorbate and the adsorbate-substrate interactions. Disordered arrangement is only activated above a critical temperature. To estimate unit-cell coverages $\theta_{\rm uc}$ we need to know, for a full ML, how many molecules cover a given area of graphene or how large an area A does one molecule cover, on average, in these experimentally observed structures.

For most of the n-alkane molecules we find the definition of 1 ML from experiments reported in the literature [17–20]. For methane, propane, and pentane we use an estimate based on a linear interpolation of the experimental data available for other values of N, $A(N) \approx 9 + 6N$ Å^2.

For the case of PE on graphene we estimate the effective unit-cell coverage $\theta_{\rm uc}$ from a vdW-DF based estimate of the PE-PE bonding distance in the PE crystal. In an earlier study [28] one of us identified the optimal PE crystal structure within a vdW-DF characterization. From that study we estimate the optimal centerline-to-

centerline distance between the polymers to be 4.5 Å. The separation of the PE polymers used in the present study is $5\sqrt{3}\,a_g \approx 21$ Å. This gives a coverage for PE $\theta_{\rm uc}^{\rm PE} \approx 4.5$ Å/21 Å ≈ 0.21.

The effective unit-cell coverages also reflect the proximity between atoms on different copies of the periodically repeated adsorbate images. Taking n-pentane as an example we find that the closest atoms sitting on two different adsorbate images is about 7.5 Å. This is at a distance where one would expect the direct vdW coupling between adsorbates in the repeated unit-cell image to become small, although that need not be the case for the coupling through substrate mediated electronic interactions [21].

C. Nonlocal correlation

The correlation energy E_c in the total energy for the vdW-DF functional is split [29]

$$E_c[n] = E_c^0[n] + E_c^{\rm nl}[n]. \tag{2}$$

into a nearly-local part E_c^0 and a part that includes the most nonlocal interactions $E_c^{\rm nl}$. All terms of (2) are functionals of the electron density n. In a homogeneous system the term E_c^0 is the correlation $E_c^{\rm LDA}$ obtained from the local density approximation (LDA), and in general [8] we approximate E_c^0 by $E_c^{\rm LDA}$.

The term $E_c^{\rm nl}$ vanishes for a homogeneous system. It describes the dispersion interaction. The form of $E_c^{\rm nl}$ is derived in Ref. 8. It is a truly nonlocal functional

$$E_c^{\rm nl}[n] = \frac{1}{2}\int\int d\mathbf{r}\, d\mathbf{r}'\, n(\mathbf{r})\phi(\mathbf{r},\mathbf{r}')n(\mathbf{r}') \tag{3}$$

given by a kernel ϕ which is explicitly stated in Ref. 8.

In GPAW the electron density $n(\mathbf{r})$ used in (3) is the so-called pseudo-electron density $n_{\rm ps}$. In the PAW scheme, this is made relatively smooth by splitting off core-like electrons in an augmentation density, $n_{\rm aug}$, i.e., writing $n = n_{\rm ps} + n_{\rm aug}$. The evaluation of semi-local functional contributions — including E_c^0 and the vdW-DF exchange — is based on the variation in $n_{\rm ps}+n_{\rm aug}$. The inclusion of parts of $n_{\rm aug}$ was recently shown to be important [26] for converging a PAW based vdW-DF implementation in the code VASP [30] in calculations of bulk lattice constants.

D. vdW-DF-based studies of adsorption energies

The adsorption energy E_a is the difference between the energy of the optimal adsorption configuration and the energy, $E_{\rm gas}^{\rm vdW\text{-}DF}$, of the system with the n-alkane molecules moved far away from graphene and far from each other in a gas form,

$$-E_a = E_{\rm near}^{\rm vdW\text{-}DF} - E_{\rm gas}^{\rm vdW\text{-}DF}. \tag{4}$$

When bonds are strong, in proper chemisorption problems, a formal definition like (4) can also be directly employed for practical computations with traditional DFT using semi-local functionals. For the reference energy $E_{\rm gas}^{\rm vdW\text{-}DF}$ one can generally take each fragments in independent unit cells of difference sizes and griding. There is for dense matter problems no important long-ranged direct interactions between repeated images of the adsorbates (or, in the direction perpendicular to the surface, between the adsorbate and repeated images of the substrate). There can be indirect substrate mediated interactions [21, 31, 32] but these are small adjustments on a chemisorption energy scale. Also, while numerical noise can arise in the calculation of exchange-energy terms in some codes [22, 33], the effects are limited. This is because it is the low-density regions which are more prone to noise [34] but in chemisorption problems one can use moderately-sized unit cells.

However, for n-alkane adsorption investigated using a DFT method like vdW-DF, we cannot directly employ (4), at least not without a discussion. We have here chosen to bypass all (small) effects of residual direct vdW coupling between adsorbate images, potential noise issues [22, 33, 34] that can arise when comparing unit cells with different large amounts of vacuum [22, 33, 34], *and* control [25, 35] a grid sensitivity/convergence issue [26] that can arise in vdW-DF calculations of energy differences.

Following Refs. 12, 22, 23, we formally rewrite the vdW-DF adsorption energy

$$-E_a = \Delta E_{\rm froz}^{\rm vdW\text{-}DF} + \Delta E_{\rm far}\,, \tag{5}$$

$$\Delta E_{\rm froz}^{\rm vdW\text{-}DF} = E_{\rm near}^{\rm vdW\text{-}DF} - E_{\rm far,froz}^{\rm vdW\text{-}DF}\,, \tag{6}$$

$$\Delta E_{\rm far} = E_{\rm far,froz}^{\rm vdW\text{-}DF} - E_{\rm gas}^{\rm vdW\text{-}DF}, \tag{7}$$

where the first difference (6) is evaluated in the same unit cell, containing both substrate and adsorbate, and with identical grid. Use of an intermediate reference energy in (6) subtracts not only intra-molecular contributions (the alkane molecule is identical in the two calculations) but also any direct lateral alkane-alkane interaction across unit cell boundaries.

In the second energy difference (7) one should, in principle [25] ensure the same grid density for the two unit cells, describing either a repeated pattern of frozen molecules or isolated molecules in the fully relaxed gas form. In practice, we approximate [12]

$$\Delta E_{\rm far} \approx E_{\rm froz}^{\rm PBE} - E_{\rm gas}^{\rm PBE}\,, \tag{8}$$

that is, in a calculation using the generalized gradient approximation (GGA) in the Perdew-Burke-Ernzerhof [36] (PBE) variant, thus also eliminating all possible direct vdW coupling in $\Delta E_{\rm far}$. The energy contribution (8) is of no real significance in the present study.

We note that some additional care must generally be exercised in vdW-DF studies since that sparse-matter binding energies are significantly smaller and thus more

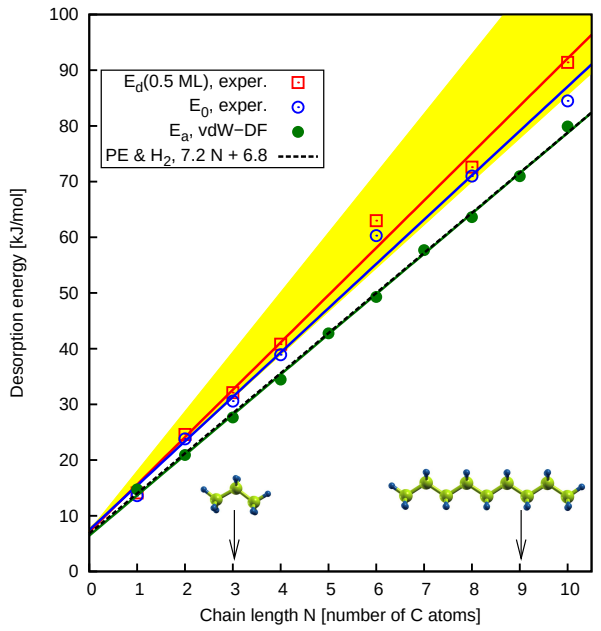

FIG. 2: Desorption energy as a function of the length of the n-alkane chain. Solid points are our results, open points are from the TPD measurements by Tait et al. [1]. Linear regression lines for the three sets of data points are also shown, including the extrapolations to $N = 0$. The dashed line has the slope from our calculations of the adsorption of PE, with the H_2 adsorption energy added to represent the ends of the alkanes. The shaded area encompasses the estimated (by Ref. 1) error bars of the 0.5 ML experimental data.

susceptible to both spurious (unit-cell) interactions and potential noise and grid effects. Several of the vdW-DF implementations are in DFT codes that were mostly created for dense-matter systems and with default convergence setting designed to determine energy scales closer to 1 eV than 1 meV; some adjustments of settings have been discussed above. It is not always a priority in the general DFT codes to converge the low-density regions which are important in accurate calculations of the vdW bonding [29, 37].

In the here-described GPAW calculations we find that a direct approach based on (4) yields no real differences when we use the same grid density for the unit cell value of $E_{\rm near}^{\rm vdW\text{-}DF}$ and $E_{\rm gas}^{\rm vdW\text{-}DF}$ [25, 35]. With the increased convergence criteria and large unit cells (Section II.A) there arises no relevant contribution from numerical noise [34] nor any sizable direct vdW coupling [21]. Nevertheless, we have chosen to stick with the earlier procedure because it also includes handling of grid density effects.

The adsorption energy may be affected by substrate-mediated electronic interactions. We provide an argument in the results section, but a full discussion is beyond the scope of this investigation.

III. RESULTS AND DISCUSSION

A. Structure and relaxations in adsorption

The alkane molecules deform very little upon adsorption, compared to their gas phase structure. In the gas phase, calculated with vdW-DF, we find for n-pentane the average C-C bond length 1.541 Å. The C-C distance varies slightly along the carbon chain, with the smallest values towards the ends and the largest values around the center of the chain, but the difference only amounts to 0.001 Å. For n-nonane the C-C bond lengths along the chain differ by 0.002 Å, again with the largest values around the center of the chain. We find similar bond lengths and bond length variations for the other alkanes.

Values of the average C-C bond length found by experiment [38] for n-alkanes with $N = 2$ to 7 are in the range 1.526 Å (n-propane) to 1.536 Å (ethane). Our results for the bond lengths thus deviate less than 1% from experiment.[2]

When an alkane molecule is adsorbed on graphene we find that the bond lengths are only slightly affected. For pentane the adsorbed molecule (Fig. 1) has an average C-C bond length 1.543 Å, a change from the gas phase by 0.002 Å (or 0.1%), and the bond lengths are still larger towards the middle of the chain (1.544 Å) compared to the bonds at the ends of the chain (1.542 Å). For the other alkanes we find the average C-C bond length in the range 1.540 Å (ethane) to 1.544 Å (octane and nonane), and for all alkanes the bonds towards the middle of the chains are longer than those at the ends.

Thus, structural changes caused by the adsorption are very small. Energetically, the changes are also very small: using PBE for the reasons stated in the previous section we find the difference in total energy $E_{\rm froz}^{\rm PBE} - E_{\rm gas}^{\rm PBE}$ approximately 2 meV (0.2 kJ/mol) per C-C bond for all the alkanes studied here.

All calculations of the adsorbed alkanes presented above are for an orientation with the alkane carbon skeleton parallel to graphene. We started out the process of optimizing the atomic positions with the carbon skeleton parallel to graphene, and all calculations reached an energetic minimum when parallel to graphene. To check if this is also the global minimum we further calculated the total energy for alkane molecules that initially were oriented with their carbon skeleton perpendicular to graphene, i.e., rotated 90° around their axis. For these, we also find a local minimum, but with a total energy larger (less favorable) than for the configuration with the backbone parallel to graphene. For example for pentane

[2] When comparing the values of the bond lengths with experiment it should be kept in mind that many exchange-correlation approximations, like the vdW-DF and also many of the GGA versions, find covalent bond lengths that can deviate up to a few percent from the experimental values.

we find that the loss of total energy going from the perpendicular orientation to the parallel orientation is 48 meV (4.6 kJ/mol).

B. Adsorption and desorption energies

Table I lists the adsorption (desorption) energies obtained from theory by us and through TPD measurements by Tait et al. [1]. As shown in Figure 2 the calculated adsorption energy values grow linearly with the size of the alkane molecule, N, with an off-set comparable to that from experiments. Although the coverage of adsorbed alkanes in our calculation is 0.2–0.3 ML the subtraction procedure involving the two first terms in (5) ensures that all direct alkane-alkane interactions are eliminated. Thus our results should be compared with experimental results for single alkane molecules desorbed from otherwise clean and defectless graphene (coverage 0 ML), E_0.

In Ref. 1, the model used for describing the desorption energy E_d as a function of the coverage θ and the number of alkane C atoms N is

$$E_d(\theta, N) = E_0(N) + \gamma(N)\theta + E_{\rm def}(N)\exp\left(-\frac{\theta}{\theta_{\rm def}(N)}\right). \quad (9)$$

The $E_0(N)$ is the contribution from a defectless surface (here: graphene) in the absence of adsorbate-adsorbate interactions. The term $\gamma(N)\theta$ accounts for the increase in desorption energy due to the interaction with other adsorbates on the surface, and the third term describes the effect of defects in the surface. The model is introduced in Ref. 6 for n-butane on MgO(100). For general (small) n-alkanes on graphite the parameters γ, $E_{\rm def}$, and $\theta_{\rm def}$ are given in Table IV of Ref. 1. In our calculations graphene is defectless and we have compensated the lateral interactions between molecules. Therefore our adsorption energies E_a should be compared with the experimental quantity E_0, listed in Table I.

In Figure 2 are shown the experimental results E_d at $\theta = 0.5$ ML, with the corresponding error estimates within the shaded area (from Table III of Ref. 1), and E_0 at zero coverage, together with our adsorption energies E_a. Comparing E_a with E_0 we find that our theory adsorption energies deviate somewhat from the experimental results, with values from theory about 10% smaller than E_0. Hexane is an exception: our vdW-DF value E_a is 18% smaller than E_0. However, for hexane the experiment deviates from the linear growth with N whereas our theory result does not.

The solid linear curves in Figure 2 are the linear regression curves for E_d, E_0, and E_a. The experimental curves are described by $E_d = 8.50N + 7.11$ (Ref. 1) and $E_0 = 7.96N + 7.46$, and we find for the theory results the relationship $E_a = 7.23N + 6.44$, all given in units of kJ/mol.

The shaded area in Figure 2 shows the estimated errors in the values of E_d as provided by Ref. 1. We expect at least similar sizes of the errors on the experimental E_0 values because E_0 is derived from E_d (via eq. (9)), which might possibly account for part of the 10% deviation between the values of E_0 and the values of our E_a. The lack of substrate for graphene in our calculations also contributes to the deviation. Previously, one of us has estimated the contribution to the binding energy from a second layer of graphene to be 3% for benzene or naphthalene adsorbed on graphene [10] and 4% for phenol on graphene [23].

The reference system for the $\Delta E_{\rm froz}^{\rm vdW\text{-}DF}$ part of the adsorption energy [eq. (6)] has the alkane molecule ∼11 Å above graphene. In our unit cells of height 23 Å this places the reference alkane molecule at ∼12 Å distance from the periodically repeated image of graphene. In the vdW-DF calculations this leads to a small interaction of the alkane molecule and the graphene in the same unit cell and a small cross-coupling to the repeated image of graphene. Removal of this effect will increase the calculated value of E_a. For n-pentane we explicitly calculate the increase in E_a to be 20 meV (1.9 kJ/mol), or 4.5% of E_a. This value is obtained by use of unit cell of height 35.15 Å and a reference calculation with a graphene-alkane-distance of ∼17.5 Å, at an increased computational cost. This effect may be another contributing part in the 10% difference between the E_0 from experiments and our E_a.

Although all direct alkane-alkane interaction of the periodically repeated images are eliminated by use of the energy difference (6) there may remain some indirect alkane-alkane interactions mediated by graphene. This effect should lead to an oscillatory correction in the estimate of E_a [32]. The oscillations have a period set by the Fermi-surface properties of graphene. However, since different n-alkanes are modeled in different coverages $\theta_{\rm uc}$ (Table I), the error introduced by indirect electronic interactions should reveal itself *both* as a shift of the slope *and* as as scatter around the slope. The fact that there is no strong scatter in the theory-predicted slope (Figure 2) suggests that the magnitude of systematic change in the E_a slope from indirect electronic interactions is not large.

Finally, we note that GPAW uses the pseudo electron density $n_{\rm ps}$ for n in (3); It is possible that including also some of the core density $n_{\rm aug}$ [26] could adjust the value of the nonlocal correlation term $E_c^{\rm nl}$.

C. Adsorption distance

In Figure 3 we show the potential energy curve for n-pentane as pentane is moved away from graphene, obtained with the vdW-DF functional. The points of the curve are obtained as described by (5), with three sets of calculations, however with the center of mass of the molecule kept fixed at the distance d above graphene. All internal atomic positions of pentane are allowed to relax.

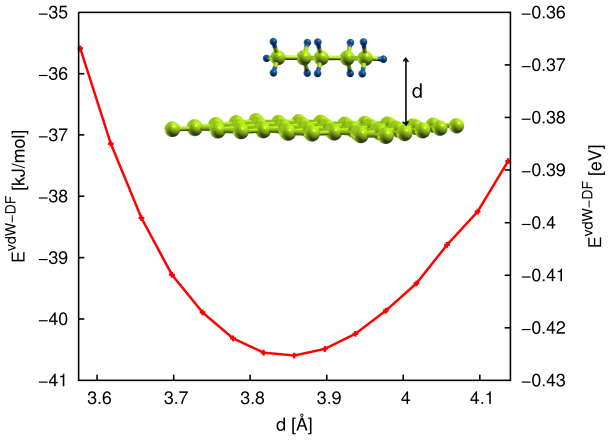

FIG. 3: Potential energy for n-pentane on graphene. The potential is calculated like $-E_a$ in (5) but with the center of mass of pentane fixed at the distances d from graphene. The minimum of the curve corresponds to the adsorption energy E_a and distance d_{cm}.

Figure 3 shows that the potential is shallow around the adsorption position. For example, moving the center of mass of pentane 0.1 Å towards or away from graphene results in an energy increase of only about 1 kJ/mol, or 10 meV. For our calculations we also report in Table I the distance d_{cm} between the center of mass of the molecule and the graphene sheet at the adsorption distance, which ranges from 3.64 Å (methane) to 3.96 Å (hexane). Because of the shallow minimum there is some uncertainty in determining d_{cm}.

D. Desorption rates and interpretations

Almost all the available experimental results on alkane desorption from various surfaces derive from TPD measurements measuring the desorption rate r. In order to extract the desorption energy from r the preexponential desorption rate ν was earlier often assumed to have the value 10^{13} s^{-1}. This value is accepted as a reasonable value for first-order processes in surface physics of atoms and is derived from traditional transition state theory. However, the more complex processes of molecular desorption are not necessarily as well described by that particular value, nor more generally by a value that is constant for all n-alkanes.

The desorption rate r may be described by the Polanyi-Wigner equation

$$r(\theta,T) = -\frac{d\theta}{dt}(\theta,T) = \nu(\theta,T)\theta^m e^{-E_d(\theta)/k_BT} \qquad (10)$$

for mth order desorption, here $m = 1$. Assuming a constant value of ν for the small ($N < 12$) n-alkanes the TPD desorption rates give linear growth in E_d with number of alkane segments N but with a very large offset [5] at $N = 0$. The offset is much larger than the segmental increment in E_d. Lei et al. speculated [39], and Tait et al. showed from analysis of TPD experiments [1, 7], that ν takes other and varying values in alkane desorption. This was shown for various surfaces like graphite, Pt(111) and MgO(100). By treating ν as a fitting parameter along with E_d, modified and varying values of ν are found. Such analysis leads to a more modest value of the offset of E_d at $N = 0$, at the size of or smaller than the segmental increment in E_d [1, 7].

In particular, it was found [1] that on graphite ν varies from $10^{13.0}$ s^{-1} for methane to $10^{17.8}$ s^{-1} for n-decane. Thus the small molecules have a desorption prefactor similar to that from theory for atoms, whereas the prefactors for the larger molecules deviate strongly from this. Taking these variations into account the desorption energy offset at $N = 0$ is reduced to 7.11 kJ/mol, with a segmental increment in E_d of 8.50 kJ/mol. Similar results were obtained for small-N n-alkane desorption from Pt(111) and MgO(100).

It appears that the previously published large values of the $N = 0$ offsets can mostly be explained [1, 6, 7] as an effect of not allowing ν to vary for the small n-alkanes. Nevertheless, an offset of a smaller size does remain even in the re-analyzed data.

In the literature the origin of the offset has been debated [1, 5, 39]. Even though the values of the offsets may be reduced as discussed above, also the remaining offset begs an explanation. Lei et al. summarize the discussions by listing a number of suggested reasons: (i) the different binding to the surface of the methyl end groups (-CH_3) compared to the methylene segments (-CH_2-); (ii) the effect from the chain length dependence on the polarizability of the alkanes; (iii) the effect of needing different temperatures for the various alkanes for measuring r; (iv) possibly the desorption process cannot be described as a first-order process, e.g., if the alkanes adsorb in islands or other structures; (v) possible lattice mismatch of the alkanes with the surface; and finally (vi) chain length dependence of ν. The latter suggestion reduces the offset to a more modest value, as discussed above.

Without going into details of all of the above-mentioned suggestions we note that our calculations are in a sense more direct than the desorption energies derived from the TPD measurements. In our calculations the preexponential factor ν is not involved, temperature variation is not an issue, and we do not let the alkanes adsorb in islands. Our results are in agreement with the results presented in Ref. 1 where the approach of a variable desorption prefactor was used. In particular, our theoretically calculated value of the offset agrees very well with that obtained by Tait et al. Here below we present a simple model study to discuss the suggestion (i) of end-group effects.

Our calculated adsorption energy for PE corresponds very well with our similarly calculated adsorption energy per segment of the alkanes (when neglecting the offset). PE is similar to the alkanes, but it does not (at least

not ideally) include methyl end groups. In our calculations we describe PE adsorbed on graphene by periodically repeating two CH_2 units, thus explicitly avoiding end groups. We find (Table I) the adsorption energy per methylene unit in PE, 7.2 kJ/mol, which corresponds very well to the energy 7.4 kJ/mol we find per (methylene or methyl) unit for small n-alkanes.

It is natural to expect that the two extra H atoms attached to the ends of the alkane molecules (in the methyl groups) also contribute to the adhesion, thus affecting the offset in the adsorption energy. We present a calculation of a H_2 molecule adsorbed on graphene to test a hypothesis of simple additivity of N methylene segments (-CH_2-) and two additional H atoms. This is thus an even simpler model for n-alkane than adding methyl to the ends of a string of methylene segments.

Our calculation of H_2 on graphene yields the adsorption energy 6.8 kJ/mol. In the calculated curve for E_a the offset is 6.44 kJ/mol. Our results for PE and H_2 fit nicely to this simple additivity model. The curve with slope derived from PE adsorption and offset derived from H_2 adsorption is plotted in Figure 2 (dashed line).

Arguments raised against the end-group explanation have been that experiments [39] for cyclic alkanes on Cu(111) and Pt(111) also show an offset for extrapolation to N even though the cyclic alkanes do not have any end groups. However, those results were extracted using fixed values of ν and yield large offsets (36 kJ/mol for Pt, 19 kJ/mol for Cu) both for the cyclic alkanes and their linear equivalents. In that analysis the effect directly on the desorption barrier from the end groups is estimated to 2 kJ/mol per linear alkane for both Pt and Cu surfaces. We cannot judge whether the value of the cyclic-to-linear difference in desorption barriers [39], 2 kJ/mol, would remain after a re-analysis of the desorption energies with more variation of ν, along the lines of those of Tait et al.

IV. SUMMARY

We present a computational study of the adsorption of small n-alkanes on graphene using the van der Waals density functional method vdW-DF. Recent desorption experiments [1] have shown desorption barriers growing linearly with the size of the alkane molecule, but with an offset in the limit of zero length. Here we reproduce in our calculations the linear dependence on the alkane length including an offset the same size as obtained by the experiments. With the help of our calculated adsorption energy of polyethylene and H_2 molecules we argue that a simple additivity assumption of alkane methylene (-CH_2-) units plus two extra H atoms for the alkane ends explains the size and origin of the energy offset very well. Summing up, our calculations thus give support to the suggestion that the offset measured in n-alkane desorption experiments (after correction for effects of varying ν) can be explained by the n-alkane end groups being different from the methylene segments of the n-alkanes.

Acknowledgments

We acknowledge discussions with Kristian Berland, Kyuho Lee, Valentino Cooper, and Per Hyldgaard. Partial support from the Swedish Research Council (VR) and from the Chalmers Area of Advance Materials is gratefully acknowledged. The computations were performed on resources provided by the Swedish National Infrastructure for Computing (SNIC) at C3SE. Mattias Slabanja is acknowledged for assistance concerning technical aspects and implementation in making the code run on the C3SE resources. EKK, ML, DO, and JDR carried out their part of the research presented here as part of the undergraduate program at Chalmers University of Technology.

[1] S.L. Tait, Z. Dohnálek, C.T. Campbell, and B.D. Kay, J. Chem. Phys. **125**, 234308 (2006).
[2] K.R. Paserba and A.J. Gellman, J. Chem. Phys. **115**, 6737 (2001).
[3] A.J. Gellman and K.R. Paserba, J. Phys. Chem. B **106**, 13231 (2002).
[4] K.R. Paserba and A.J. Gellman, Phys. Rev. Lett. **86**, 4338 (2001).
[5] Please find discussions and citations in Ref. 1.
[6] S.L. Tait, Z. Dohnálek, C.T. Campbell, and B.D Kay, J. Chem. Phys. **122**, 164707 (2005).
[7] S.L. Tait, Z. Dohnálek, C.T. Campbell, and B.D Kay, J. Chem. Phys. **122**, 164708 (2005).
[8] M. Dion, H. Rydberg, E. Schröder, D.C. Langreth, and B.I. Lundqvist, Phys. Rev. Lett. **92**, 246401 (2004); **95**, 109902(E) (2005).
[9] T. Thonhauser, V.R. Cooper, S. Li, A. Puzder, P. Hyldgaard, and D.C. Langreth, Phys. Rev. B **76**, 125112 (2007).
[10] S.D. Chakarova-Käck, E. Schröder, B.I. Lundqvist, and D.C. Langreth, Phys. Rev. Lett. **96**, 146107 (2006).
[11] S.D. Chakarova-Käck, A. Vojvodic, J. Kleis, P. Hyldgaard, and E. Schröder, New J. Phys. **12**, 013017 (2010).
[12] K. Berland, S.D. Chakarova-Käck, V.R. Cooper, D.C. Langreth, and E. Schröder, J. Phys.: Condensed Matters **23**, 135001 (2011).
[13] Open-source, grid-based PAW-method DFT code GPAW, `http://wiki.fysik.dtu.dk/gpaw/` ; J.J. Mortensen, L.B. Hansen, and K.W. Jacobsen, Phys. Rev. B **71**, 035109 (2005).
[14] J. Enkovaara et al., J. Phys.: Condens. Matter **22**, 253202 (2010).
[15] G. Román-Pérez and J.M. Soler, Phys. Rev. Lett. **103**, 096102 (2009).
[16] A. Kokalj, Comp. Mater. Sci. **28**, 155 (2003). Code available from `http://www.xcrysden.org/`
[17] F.Y. Hansen, R. Wang, H. Taub, H. Shechter, D.G. Reichel, H.R. Danner, and G.P. Alldredge, Phys. Rev. Lett. **53**, 572 (1984).

[18] K.W. Herwig, J.C. Newton, and H. Taub, Phys. Rev. B **50**, 15287 (1994).

[19] T. Arnold, R.K. Thomas, M.A. Castro, S.M. Clarke, L. Messe, and A. Inaba, Phys. Chem. Chem. Phys. **4**, 345 (2002).

[20] A. Inaba, S.M. Clarke, T. Arnold, and R.K. Thomas, Chem. Phys. Lett. **352**, 57 (2002).

[21] K. Berland, T.L. Einstein, and P. Hyldgaard, Phys. Rev. B **80**, 155431 (2009).

[22] S.D. Chakarova and E. Schröder, Mater. Sci. Engin. C **25**, 787 (2005).

[23] S.D. Chakarova-Käck, Ø. Borck, E. Schröder, and B.I. Lundqvist, Phys. Rev. B **74**, 155402 (2006).

[24] P.E. Blöchl, Phys. Rev. B **50**, 17953 (1994).

[25] E. Ziambaras, J. Kleis, E. Schröder, and P. Hyldgaard, Phys. Rev. B **76**, 155425 (2007).

[26] J. Klimeš, D.R. Bowler, and A. Michaelides, Phys. Rev. B **83**, 195131 (2011).

[27] M.S. Couto, X.Y. Liu, H. Meekes, and P. Bennema, J. Appl. Phys. **75**, 627 (1994).

[28] J. Kleis, B.I. Lundqvist, D.C. Langreth, and E. Schröder, Phys. Rev. B **76**, 100201(R) (2007).

[29] D.C. Langreth, M. Dion, H. Rydberg, E. Schröder, P. Hyldgaard, and B.I. Lundqvist, Intern. J. of Quantum Chem. **101**, 599 (2005).

[30] The Vienna Ab initio Simulation Package VASP, `http://www.vasp.at/` ; G. Kresse and J. Furthmüller, Phys. Rev. B, **54**, 11169 (1996).

[31] J. Repp, F. Moresco, G. Meyer, K.H. Rieder, P. Hyldgaard, and M. Persson, Phys. Rev. Lett. **85**, 2981 (2000).

[32] P. Han and P.S. Weiss, Surf. Sci. Rep. **67**, 19 (2012).

[33] E. Londero and E. Schröder, Phys. Rev. B **82**, 054116 (2010).

[34] E. Londero and E. Schröder, Computer Physics Communications **182**, 1805 (2011).

[35] J. Kleis, E. Schröder, and P. Hyldgaard, Phys. Rev. B **77**, 205422 (2008).

[36] J.P. Perdew, K. Burke, and M. Ernzerhof, Phys. Rev. Lett. **77**, 3865 (1996); **78**, 1396(E) (1997).

[37] H. Rydberg, M. Dion, N. Jacobson, E. Schröder, P. Hyldgaard, S.I. Simak, D.C. Langreth, and B.I. Lundqvist, Phys. Rev. Lett. **91**, 126402 (2003).

[38] NIST Computational Chemistry Comparison and Benchmark Database, NIST Standard Reference Database Number 101, Release 15b, August 2011, Editor: Russell D. Johnson III, `http://cccbdb.nist.gov/`

[39] R.Z. Lei, A.J. Gellman, and B.E. Koel, Surf. Science **554**, 125 (2004).